Structure and Composition of CO_2/H_2 and $CO_2/H_2/C_3H_8$ Hydrate in Relation to Simultaneous CO_2 Capture and H_2 Production

Rajnish Kumar
Dept. of Chemical and Biological Engineering, University of British Columbia, Vancouver, BC, Canada V6T 1Z3, and Steacie Institute for Molecular Sciences, National Research Council Canada, Ottawa, ON, Canada K1A 0R6

Peter Englezos
Dept. of Chemical and Biological Engineering, University of British Columbia, Vancouver, BC, Canada V6T 1Z3

Igor Moudrakovski and John A. Ripmeester
Steacie Institute for Molecular Sciences, National Research Council Canada, Ottawa, ON, Canada K1A 0R6

DOI 10.1002/aic.11844
Published online May 6, 2009 in Wiley InterScience (www.interscience.wiley.com).

Gas hydrates from a (40/60 mol %) CO_2/H_2 mixture, and from a (38.2/59.2/2.6 mol %) $CO_2/H_2/C_3H_8$ mixture, were synthesized using ice powder. The gas uptake curves were determined from pressure drop measurements and samples were analyzed using spectroscopic techniques to identify the structure and determine the cage occupancies. Powder X-ray diffraction (PXRD) analysis at −110°C was used to determine the crystal structure. From the PXRD measurement it was found that the CO_2/H_2 hydrate is structure I and shows a self-preservation behavior similar to that of CO_2 hydrate. The ternary gas mixture was found to form pure structure II hydrate at 3.8 MPa. We have applied attenuated total reflection infrared spectroscopic analysis to measure the CO_2 distribution over the large and small cavities. ^{1}H MAS NMR and Raman were used to follow H_2 enclathration in the small cages of structure I, as well as structure II hydrate. © 2009 American Institute of Chemical Engineers *AIChE J,* 55: 1584–1594, 2009

Introduction

CO_2 and H_2 are known to form gas hydrates but under considerably different conditions. Carbon dioxide forms structure I (sI) hydrate at moderate pressures, e.g., in the range of a few MPa[1] at 273 K. On the other hand, H_2 forms structure II (sII) hydrate at a very high pressure of ~200 MPa.[2,3] It has been reported that at such high pressures a cluster of up to two H_2 molecules occupies the small hydrate cages, whereas the large cages may have clusters of up to four H_2 molecules. The difference in hydrate formation pressure of CO_2 and H_2 hydrates has been exploited to preferentially incorporate CO_2 in the hydrate cages from a CO_2/H_2 mixture, thus, partitioning the gas components. A 40/60 mol % CO_2/H_2 mixture is known as a fuel gas mixture, because it is the product gas from a gasification/shift reactor process plant, and is available at pressures between 2.5 and 5 MPa.[4,5] Previous work in our laboratory has demonstrated that clathrate hydrate crystal formation can be used as a separation process for the capture of CO_2.[6–9]

Based on hydrate phase equilibrium studies and gas uptake measurements (kinetic) on hydrate formation from the 40/60 mol % CO_2/H_2 gas mixture, it was concluded that H_2 occupies the hydrate phase.[10,11] This observation is in agreement with the work by Kim and Lee[12] in which it was shown that a 20/80 mol % CO_2/H_2 gas mixture forms structure I hydrate and H_2 is included in the hydrate. On

Additional Supporting Information may be found in the online version of this article.

Correspondence concerning this article should be addressed to P. Englezos at englezos@interchange.ubc.ca

the other hand Sugahara et al.[13,14] reported that H_2 behaves like a diluent gas, and, thus, does not take part in hydrate formation.

Because the hydrate formation pressure for the CO_2/H_2 mixture (40/60 mol %) is high for the CO_2/H_2 separation process, the addition of 2.6 mol % C_3H_8 was evaluated.[9,10] This reduces the hydrate formation pressure substantially, and, hence, the associated compression costs without compromising the separation efficiency. Studies on the impact of additives on hydrate formation from H_2 or H_2/CO_2 mixtures have been primarily motivated from the interest in hydrogen storage. Florusse et al.[15] reported that hydrate clusters of H_2 could be stabilized and stored at low-pressure in sII binary clathrates. Clusters of up to two H_2 molecules occupied small water cages, whereas large water cages are singly occupied by tetrahydrofuran (THF). Lee et al.[16] suggested that by tuning the composition of THF and H_2 in a hydrate forming mixture, it is possible that H_2 occupies both cages i.e., some of the larger and the smaller cages of the resultant sII hydrate. Hasimoto et al.[17] reports sII hydrate formation from CO_2/H_2/THF hydrate, with H_2 and CO_2 occupying the small cages and THF going into the large cages. It must be noted that, the exact capacity of the hydrate cages for H_2 is still controversial.[18] Several studies done on THF/H_2 hydrate point toward single occupancy of hydrogen in the small hydrate cages, whereas multiple hydrogen was found to occupy the large cages.[19–22] Lokshin et al.[19] performed neutron diffraction studies on the simple D_2 (deuterated H_2) hydrate, however, contrary to the work of Mao et al.[2,3] Lokshin et al.[19] found only one hydrogen molecule in the small cavities of resultant sII hydrate. The large cavity occupancy was found to vary between two and four H_2 molecules depending on the synthesis pressure and temperature. A detailed account of cage occupancy in simple and binary hydrates of H_2, and storage capacity of these hydrates is presented by Strobel, 2008.[23]

As mentioned previously, indirect observations through kinetic and equilibrium studies on the hydrate formed by a (40/60) mol % CO_2/H_2 mixture and (38.2/59.2/2.6) mol % $CO_2/H_2/C_3H_8$ mixture showed that H_2 participates in hydrate formation. Therefore, the objective of this work is to determine the structure and cage occupancies of the hydrates formed by the CO_2/H_2 and the $CO_2/H_2/C_3H_8$ gas mixtures by employing analytical techniques like powder-XRD, Raman, Infrared and NMR spectroscopies. This information will aid in the further development of the clathrate process for simultaneous precombustion capture/hydrogen production.

The determination of the cage occupancies for the mixed hydrates in this study represents considerable challenges. As mentioned earlier, the exact capacity of the hydrate cages for H_2 is still controversial.[18] Whereas initial work claimed two H_2 per small cage,[2,24,25] neutron powder diffraction results have been interpreted in terms of a single H_2 per cage.[19,21] This result has influenced the interpretation of other data, such as gas release measurements, which, of course can give no direct information on actual cage occupancy, although it can give an average value. Modeling calculations have shown support for both single and double occupancy of the small cage.[26] One reason why it has been difficult to confirm the occupancy limits of the hydrate cages is that so far there are no reliable direct methods. Powder diffraction is limited by the data/parameter ratio in fitting any but the simplest models, Raman spectroscopy is not quantitative, as scattering cross sections for the different cavities remain unknown and there is also ortho-para conversion, making the spectrum time-dependent on the scale of days to weeks.[27] On the NMR side, the calculated chemical shift scale for H_2 is very small, and again there are problems with ortho-para spin conversion.[27,28] The problem is further complicated by the fact that hydrogen diffuses rather easily through the six rings of hydrate cages, less readily through the five rings, so that the detailed temperature history of a sample becomes important for all methods of analysis.[28,29]

For CO_2 cage occupancies there are also some difficulties. Raman spectroscopy does not distinguish CO_2 in large and small cages,[30] and for NMR spectroscopy it is not completely straightforward either as one must use the anisotropic chemical shift patterns. Infrared spectroscopy does offer opportunities, and we explore a new approach, FTIR attenuated total reflection (ATR) spectroscopy *in situ* at high-pressure to distinguish CO_2 in large and small cavities. The combined results offer a reasonably complete picture of the guest distribution and the utility of the hydrate approach to separating CO_2 from H_2.

Experimental Section

A (40/60) mol % (CO_2/H_2), and a (38.2/59.2/2.6) mol % $CO_2/H_2/C_3H_8$ were used. Approximately five grams of fresh-ground ice particles ($d < 63$ μm) were poured by gravity into a 50 mL pressure vessel (reactor). Ice was ground at liquid nitrogen temperature, and the particle size was determined by passing the ground ice through an ASTM 230 sieve at -20°C. The loading procedure was performed in a freezer at -20°C to prevent melting of the ice. The vessel was then immersed in a constant temperature water-methanol (50:50 by mass) bath and connected to a valve and pressure transducer. Before the start of the experiment the vessel was evacuated to eliminate the presence of air. The time-zero of the measurement was recorded as the vessel was pressurized to the desired pressure of 8.0 MPa (for CO_2/H_2 mixture) at -20°C and 3.8 MPa for the $CO_2/H_2/C_3H_8$ mixture. All experiments were performed at -20°C for about 24 h. At the end of the 24 h period the temperature was increased to a point above the ice point (1°C) within 5 min to enhance the conversion of ice into hydrate. It is well known that temperature ramping enhances the conversion to hydrate.[27] The temperature was then brought back to -20°C for further hydrate formation. The starting pressures were well above the stability region of sI hydrate to ensure there was sufficient driving force for hydrate formation. As the experiment was conducted in batch mode, the pressure decreased continuously as hydrate formed. The, final pressure was $\sim$1.0 MPa lower than the starting pressure. The experiments were stopped when a significant pressure drop was no longer observed. The moles of gas uptake over time were calculated from the pressure drop data by following a method given elsewhere.[11] Hydrate samples were collected under liquid nitrogen temperature (~ -190°C) at the end of the experiment and kept in liquid nitrogen for subsequent analysis.

Crystal structures and lattice constants were obtained from powder X-ray diffraction (PXRD). The PXRD measurements

were performed by a $\theta/2\theta$ step-scan mode, with a counting time of 47.3 s/step, and a step width of 0.041° in the 2θ range of 5–60°C (40 kV, 40 mA; BRUKER axs model D8 Advance). The PXRD measurements were done using Cu-Kα radiation ($\lambda = 1.5406$ Å) at −110°C to prevent hydrate dissociation. The temperature deviation of the sample during measurement was within ±1.0°C.

^{1}H and ^{13}C NMR measurements were carried out on a Bruker DSX-400 NMR spectrometer (magnetic field of 9.4 T). The ^{1}H and ^{13}C Larmor frequencies were 400.1 and 100.63 MHz, respectively. A BL7 MAS probe with stretched spinners was used. Hydrate samples were kept and loaded into the spinners in liquid nitrogen. All the NMR measurements were performed at spinning speed of 2,500–4,000 Hz at −110°C maintained by a Bruker BT 3000 temperature controller. ^{13}C data were acquired in Bloch decay mode (^{13}C $\pi/2$ pulse of 5 μs) with high-power composite pulse proton decoupling. The delay between the scans was set at 80–100s, which was sufficient for a complete relaxation of all the signals and the quantitative measurements. 100 and 300 scans were commonly acquired to obtain sufficient signal-to-noise ratio. Due to a strong proton background signal, the ^{1}H spectra were acquired as spin-echoes synchronized with the rotation of the sample. Because of this procedure, quantitative intensity measurement required accurate T_2 (spin-spin relaxation time) measurement for each resonance. Only 16 or 32 scans were required for a good signal-to-noise ratio. For absolute quantitative measurements a sample of THF hydrate of known composition was used as a quantitative standard, and its ^{1}H and ^{13}C spectra were obtained under conditions identical to those used for the hydrates studied. All of the acquisition parameters were set to ensure that the measurements were quantitatively accurate. Tetramethylsilane was used as an external chemical shift reference for both ^{13}C and ^{1}H.

The hydrate samples were also analyzed using Raman spectroscopy. An Acton Raman spectrograph with fiber optics and equipped with a 1,200 grooves/mm grating and an externally cooled CCD detector was used in this study. An Ar-ion laser was used as the excitation source emitting at 514.53 nm. The laser was focused on the sample by 10x microscope objective on a sample area of 2-3 μm^2. The spectrograph was controlled with a computer and the spectra were recorded with a 1s integration time over 100 to 500 scans. In order to determine the composition of the gas phase and the gas evolved from the decomposition of the hydrate sample at the end of the experiment, an SRI 8610 C gas chromatograph (GC) is used.

In order to monitor the mass numbers of effluent gas from a decomposing hydrate sample at atmospheric pressure, an MKS Instruments Cirrus quadrupole mass spectrometer with a heated capillary inlet line was used. Finally, a Fourier transform infrared spectrometer (FTIR) coupled with an attenuated total reflection (ATR) optical unit, was used for analyzing hydrate samples. The supercritical fluid analyzer version of a Specac Golden Gate® diamond ATR unit was slightly modified to synthesize the hydrate and analyze it *in situ*. The stainless steel sample chamber of this ATR cell is capable of withstanding pressures up to 40 MPa and can be coupled with a variable temperature unit. The stainless steel sample cell has a volume of 28 μL. A water droplet of volume less than 28 μL is placed in the cell which flattens under the gas pressure and then forms a thin hydrate film on the diamond surface. This hydrate layer was allowed to grow for two hours before the temperature was lowered to −50°C from the hydrate formation temperature (−20°C). This thin film of hydrate was stable at this temperature and could be analyzed by FTIR. The peaks for CO_2 in the small and large cages were obtained with 50 scans in order to get a good signal-to-noise ratio. Spectra were acquired from 500 to 4,000 cm^{-1} with a nominal resolution of 1 cm^{-1}.

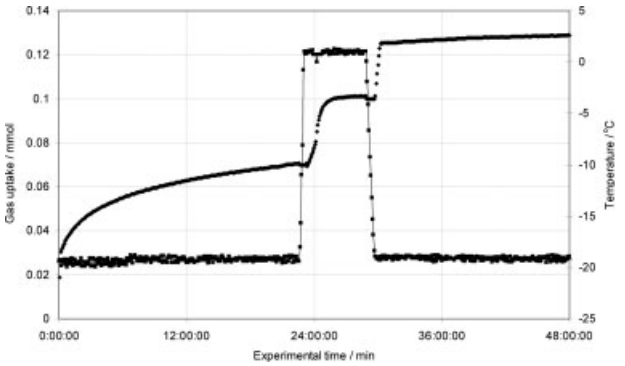

Figure 1. Gas uptake profile during hydrate formation from ice powder and the CO_2/H_2 mixture synthesized at 8 MPa.

Results and Discussion

Figure 1 shows a typical plot of the gas consumed (left axis) vs. time during hydrate formation. This is the typical and well known gas uptake curve and is considered to correlate with hydrate crystal growth. The temperature is also shown on the right axis. As seen, a period of rapid hydrate growth during the first two hours is followed by a more gradual decrease in pressure: because of this pressure drop the driving force diminishes (driving force can be excess pressure at constant temperature, or subcooling at constant pressure). Also, a hydrate film will have covered the ice surface,[31] thus, the reaction became limited by the diffusion of guest gas molecules across the hydrate film and the reaction at the ice-hydrate interface. The ramping of temperature above the ice point increased the pressure before this dropped back down again. As the temperature increases above the melting point of ice the rate of hydrate growth increases considerably. This phenomenon is well known and is due to the melting of the ice, which in turn induces fracturing of the hydrate layer, and this allows better contact between gas and water or ice.[32–34] It is also seen that the rate of gas consumption becomes constant after some time, most likely due to a decreased driving force, which can be brought back to higher values by reducing the temperature to −20°C, and which results in additional hydrate being formed. Based on the gas uptake measurement the conversion of the ice to hydrate was found to be approximately 95%. This result was confirmed from the ice peak intensities shown in the powder-XRD pattern.

Figure 2 shows the X-ray powder diffraction pattern for hydrate synthesized from the CO_2/H_2 mixture. The hydrate

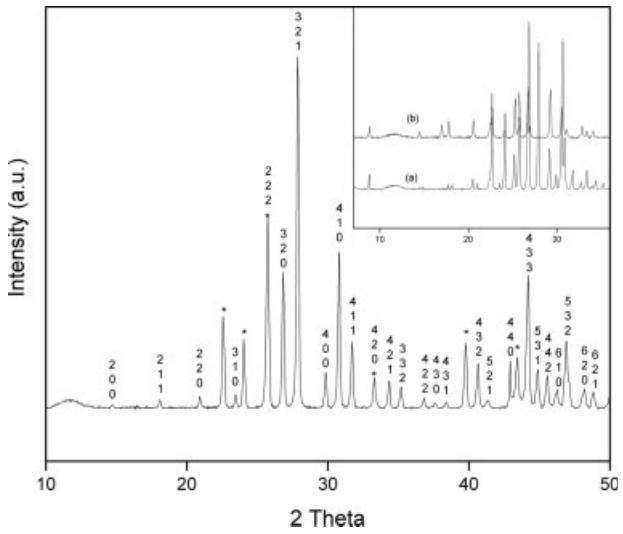

Figure 2. The X-ray diffraction pattern of the (40/60 mol%) CO_2/H_2 hydrate.

The X-ray powder diffraction data were collected at −110 °C and atmospheric pressure. CO_2/H_2 forms sI hydrate at 8.0 MPa, whereas the $CO_2/H_2/C_3H_8$ mixture forms hydrate of sI & sII at 5.0 MPa (a), and only sII hydrate at 3.8 MPa (b). The composition of the $CO_2/H_2/C_3H_8$ gas mixture is given in Table 1.

sample analyzed at −110°C and atmospheric pressure can be indexed in the regular cubic space group *Pm3n*, with a unit cell parameter of 11.89 (±0.01) Å and cell volume of 1681 (±10) cubic Å. This result matches with the reported values for the unit cell parameter of pure structure I CO_2 clathrate hydrate.[35] The presence of ice is indicated by the asterisk on top of the ice reflections. It was found that this gas mixture always formed structure I hydrate under the temperature and pressure conditions used.

The powder-XRD pattern obtained from the hydrate formed with the ternary $CO_2/H_2/C_3H_8$ (38.2/59.2/2.6 mol %) mixture is shown as an insert in Figure 2. Figure 2a shows the powder pattern of the synthesized hydrate at 5.0 MPa, whereas Figure 2b shows the pattern of the hydrate synthesized at 3.8 MPa. The powder patterns show that the hydrate formed at 5.0 MPa is a mixture of structure I and structure II hydrate, whereas that at 3.8 MPa is pure structure II hydrate. It is noted that hydrates in both cases were synthesized for 20 h at −20°C, followed by 4 h at 1°C, and then bringing back the temperature to −20°C for another 20 h. Additional experiments were performed during which hydrate samples were formed and analyzed after two and ten hours. These additional experiments confirmed the above structural findings which are consistent with expectations from thermodynamics. Thus, when the hydrate is synthesized at 3.8 MPa, thermodynamically it is possible to form only structure II hydrate with propane occupying the large cages. However, when the $CO_2/H_2/C_3H_8$ mixture is used for hydrate formation at 5 MPa and −20°C, thermodynamically it is possible to form structure I (with only CO_2 and H_2 occupying the hydrate cages) and structure II (with all the three gases occupying the hydrate cages) hydrate.

It was found that C_3H_8 preferentially occupies the large cage of sII and tends to enhance the stability of the hydrate. However, the Langmuir constant for CO_2 in the large cage of structure I is greater than it is for that of sII. Thus, CO_2 would preferentially occupy the large cage of sI over that of sII for the same fugacity of CO_2 in the vapor phase. It is also more efficient for CO_2 to occupy the large cages of structure I, as sI has more large cages than sII for a given volume, and, hence, there is a greater opportunity for CO_2 to become incorporated in the large cages of sI. Therefore, at 5 MPa a hydrate which is a mixture of structure I and structure II forms. It is important to note that all the hydrates of $CO_2/H_2/C_3H_8$ analyzed for characterization purpose were synthesized at 3.8 MPa to ensure that the hydrate is pure structure II. It would be impossible to characterize the composition and cage occupancy of a hydrate mixture without knowing the amounts of sI and sII.

Figure 3 shows the PXRD pattern of the dissociating hydrate of CO_2/H_2 (from structure I to ice) as temperature is increased from −110°C to 5°C in steps of 5°C with a 2θ scan time of 2.5 minute. The rate of increase in temperature was approximately 2.0°C per minute during the diffraction test. Peak intensities assigned for ice increase with temperature and the peak intensity assigned to hydrate becomes smaller. This indicates that dissociating hydrate is transformed into ice. The insert in Figure 3 shows the intensity ratio of the hydrate peaks (2θ from 20 to 32) at any time to the hydrate peaks at zero time as a function of temperature. It can be seen from the insert that the hydrate obtained from the CO_2/H_2 mixture with or without C_3H_8 starts decomposing at approximately −100°C. In the case of the $CO_2/H_2/C_3H_8$ hydrate (structure II) the dissociation of hydrate proceeds in one step up to around −60°C where all the hydrate has been completely transformed into ice. However, the dissociation of CO_2/H_2 hydrate (structure I) proceeds in stages. It was also interesting to note that there was almost 40% hydrate left at −10°C, which only decomposed completely once the temperature reached the melting point of ice. The

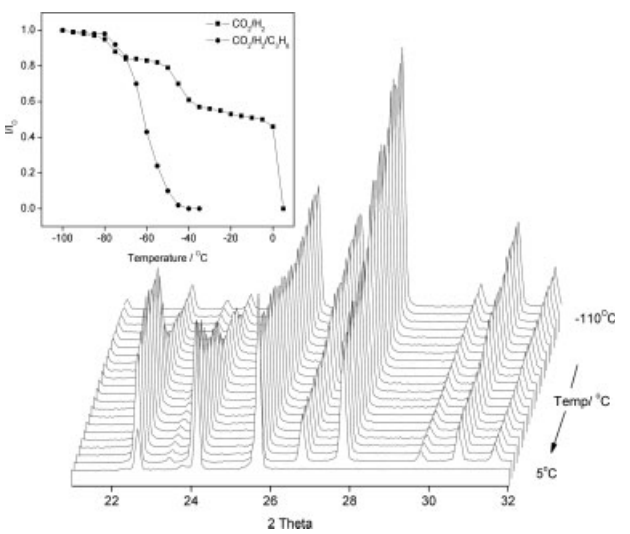

Figure 3. Temperature-dependent PXRD profile for (40/60 mol%) CO_2/H_2 hydrate from −110°C to 5 °C.

Inset shows intensity ratio of hydrate peak as a function of temperature during transformation of CO_2/H_2 hydrate (8 MPa & −20°C,) and $CO_2/H_2/C_3H_8$ hydrate (3.8 MPa & −20°C) into ice.

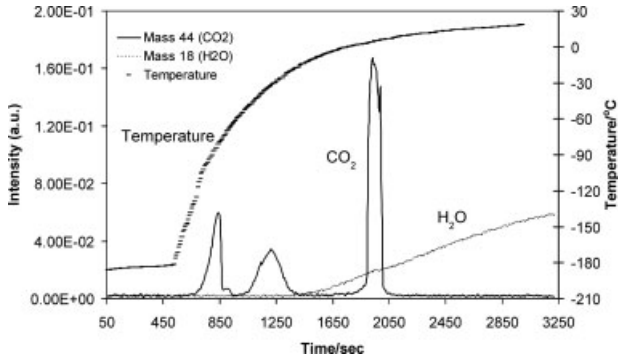

Figure 4. The mass signatures of CO_2 and H_2O released from a dissociating CO_2/H_2 (40/60 mol %) hydrate subjected to a temperature increase.

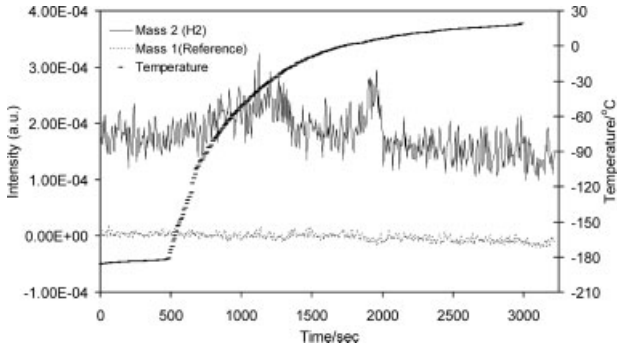

Figure 5. The mass signature of H_2 gas released from a dissociating (40/60 mol%) CO_2/H_2 hydrate subjected to a temperature increase.

Mass number 2 is for hydrogen leaving the hydrate lattice on decomposition, mass 1 is shown as a reference.

aforementioned observation matches well with the self-preservation phenomena reported in the literature for CO_2 hydrate.[36]

Stepwise dissociation of CO_2/H_2 hydrate is possible if the hydrate synthesized is actually a mixture of pure CO_2 hydrate (structure I) and CO_2 & H_2 hydrate (structure I). If such a hydrate sample stored at liquid nitrogen temperature were decomposed by gradually heating the hydrate at atmospheric pressure, it is expected that CO_2/H_2 hydrate would decompose at lower-temperature (being less stable compared to pure CO_2 hydrate) compared to pure CO_2 hydrate. In order to examine whether the hydrate synthesized from CO_2 and H_2 was a mixture of pure CO_2 hydrate and hydrate of CO_2/H_2 a sample was decomposed at atmospheric pressure by gradually increasing the temperature and allowing the gas evolved to pass through a mass spectrometer with a heated capillary inlet line. Figures 4 and 5 show the gas obtained from the decomposition of the hydrate as a function of time. The temperature is also shown. As seen in Figure 4, the first peak of carbon dioxide appears at about $-80°C$, which coincides with the melting point of dry ice. Dry ice is accumulated in the system when a hydrate reactor pressurized with the CO_2/H_2 mixture is quenched at liquid nitrogen temperature to recover the hydrate. As seen in Figure 4, CO_2 release stops until the temperature of hydrate sample is increased to $-55°C$. At temperatures close to $-30°C$ a peak corresponding to the CO_2 from the decomposed hydrate is seen. However, as the temperature increases further, CO_2 release is not observed until the temperature reaches close to 0°C, where another CO_2 peak is seen. It is likely that due to the self-preservation effect hydrates are kinetically stable above the theoretical equilibrium point and a portion of the hydrate decomposes close to 0°C. Figure 4 also shows that water vapor can be detected at a temperature as low as $-15°C$. Figure 5 shows the pattern of hydrogen escaping from the hydrate cages. The temperature dependence of species with mass number 1 is also plotted in Figure 5, which acts as a reference line for mass 2 (H_2). The amount of hydrogen present in the hydrate cages is at least an order of magnitude less than CO_2, hence; a relatively smaller peak for H_2 is seen. However, it is evident that hydrogen release also follows the decomposition pattern shown by CO_2 since the majority of H_2 from the hydrate phase accompanies CO_2, once at $-60°C$ and then again at a temperature closer to the melting point of ice. These observations indicate that the hydrate synthesized and analyzed was a CO_2/H_2 hydrate. We note that this H_2 release pattern is quite different than those for sII mixed hydrates ($CO_2/H_2/C_3H_8$ mixture). In the latter hydrate, the small cavities form continuous layers by face sharing of the D cages (5^{12} cages), thus, a continuous diffusion path is available for hydrogen to leave the hydrate.[28] In sI hydrate, the small cavities are surrounded by the T cages ($5^{12}6^2$ cages), which contain CO_2 molecules, thus, blocking diffusion pathways for H_2.[29] Moreover, the hydrate exhibits the self-preservation effect similar to that for CO_2 hydrate,[36] thus, it is possible to store H_2 quite effectively in sI hydrate, although there is far less capacity because of the small number of D cages. Once the PXRD and mass spectroscopic measurements confirmed that the solid phase contained homogeneous hydrate, the hydrate phase composition was obtained by gas chromatography. Table 1 shows the gas/hydrate composition at each stage for both systems. This result is in agreement with the gas uptake measurement

Table 1. Phase Composition at Start and End of the Experiment as Analyzed by Gas Chromatography

Description	CO_2 (mol%)	H_2 (mol%)	C_3H_8 (mol%)
CO_2/H_2 mixture			
Feed gas composition (start)	40.1 (±0.1)	59.9 (±0.1)	–
Gas phase composition (end)	20.0 (±0.2)	80.0 (±0.2)	–
Hydrate phase composition	91.8 (±0.2)	8.2 (±0.2)	–
$CO_2/H_2/C_3H_8$ mixture			
Feed gas composition (start)	38.2 (±0.2)	59.2 (±0.2)	2.6 (±0.2)
Gas phase composition (end)	23.2 (±0.2)	76.4 (±0.2)	0.4 (±0.2)
Hydrate phase composition	74.2 (±0.2)	11.2 (±0.2)	14.6 (±0.2)

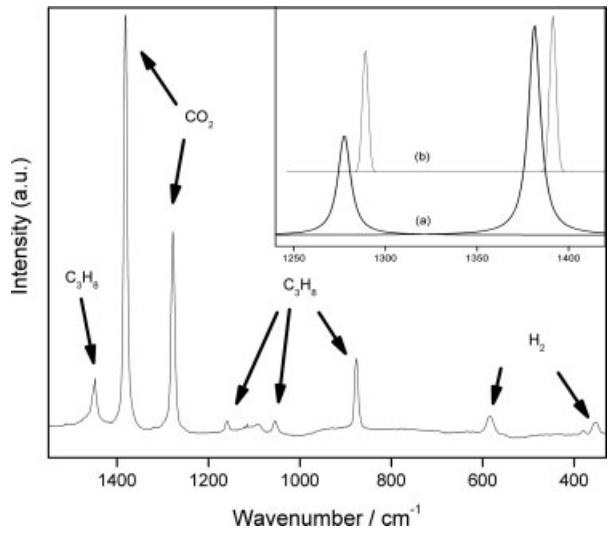

Figure 6. Raman spectrum for the Fermi diad of CO_2 incorporated into hydrate phase from the $CO_2/H_2/C_3H_8$ gas mixture.

Note the rotational mode of H_2 occupying the hydrate cages and several C-C stretching modes of C_3H_8. The figure in the inset suggests the broadening and redshift of CO_2 incorporated in hydrate phase (a) compared to CO_2 in gas phase (b).

performed on the similar system[9,11] at a temperature above the melting point of ice and pressure similar to the one reported here.

Raman spectra for the rotational and vibrational stretching regions (vibrons) of hydrogen were recorded to find the signature of hydrogen in the hydrate cages. The low-frequency spectra from hydrogen are usually dominated by the rotational excitations of the hydrogen molecules which appear at 300–850 cm^{-1}. The vibron (molecular vibration) region for hydrogen in the hydrate phase appears at 4,100–4,200 cm^{-1}. Figure 6 shows a typical Raman spectrum from the $CO_2/H_2/C_3H_8$ sII hydrate synthesized at 3.8 MPa. The spectrum was obtained by focusing the laser on the solid hydrate phase at atmospheric pressure and liquid nitrogen temperature. The signatures of all the three gases in the hydrate phase are seen. Hydrogen rotational bands in the hydrate phase can be seen at 355 cm^{-1} and 585 cm^{-1}.[18] It has to be noted that hydrogen from the gas phase appears at 359 cm^{-1} and 590 cm^{-1} (not shown). This suggests that the peaks associated with the hydrogen rotational bands are redshifted in the hydrate phase by almost 5 cm^{-1}, and that these frequencies are not greatly perturbed for hydrogen in the cages. Raman frequencies for gases trapped in the hydrate phase are generally shifted (propane is an exception) to lower wave numbers, as in the case of CO_2, shown as an insert in Figure 6. The two largest peaks, one at 1,278 cm^{-1}, and the other 1,382 cm^{-1} in Figure 6 correspond to the Fermi diad of CO_2 in the hydrate cages. Figure 6a shows the Fermi diad positions of CO_2 in the hydrate phase, and 6b shows the Fermi diad positions of CO_2 in the gas phase. It has been reported previously that Raman spectra for pure CO_2 hydrate do not show peak splittings[30] even though CO_2 occupies both the small and large cages.[37] Peak splitting has been observed with infrared spectroscopy[38] and this is discussed later in this article. Propane shows several peaks in the C-C stretching region and the most prominent one appears at about 878 cm^{-1} (Figure 6). Propane only occupies the large cage of structure II hydrate, and, hence, does not show any peak splitting for guests in different cages. It is noted that CO_2/H_2 hydrate, which forms structure I also shows similar Raman spectra (not shown) in this region. The peak positions for CO_2 and H_2 in structure I and structure II hydrate remain unchanged (within ± 1 wave number).

Figure 7 shows Raman spectra in the hydrogen vibron region of the gas and the hydrate phases. Hydrogen gas at ambient conditions shows four visible peaks $Q_1(0)$, $Q_1(1)$, $Q_1(2)$, and $Q_1(3)$ which appear at 4,161, 4,155, 4,144, and 4,126 cm^{-1}, respectively. The even number in parenthesis denotes the para- state of hydrogen (total nuclear spin of zero) whereas the odd number denotes the ortho- state of hydrogen (total nuclear spin of 1). Under ambient conditions, the ratio of ortho- to para- hydrogen is 3:1, which results in a larger ortho- peak at 4,155 cm^{-1} compared to para- peak at 4,161 $cm-^{1}$ (H_2 gas in Figure 7). However, at liquid nitrogen temperatures at equilibrium the ratio of ortho hydrogen to para hydrogen is close to 1:1.[28] In the hydrate phase the H_2 signature appears as a doublet with maxima at 4,120 cm^{-1} and 4,126 cm^{-1}. The shift to lower frequency for each Q band in the hydrate phase is attributed to changes in the H-H stretching mode when H_2 is enclathrated.[15] Moreover, the H_2 vibron bands at 4,120 and 4,126 cm^{-1} consist of relatively broad peaks typical of enclathrated guests in the hydrate cavities. The enclathrated hydrogen gives rise to a strong signal even at atmospheric pressure and $\sim -190°C$, owing to its higher density of H_2 in the hydrate phase. It is clear from Figure 7 that in the presence of help gases like CO_2 and C_3H_8, H_2 occupies the small cages of structure I and II hydrate, respectively, even at moderate pressures (further information is provided in the supplementary section).

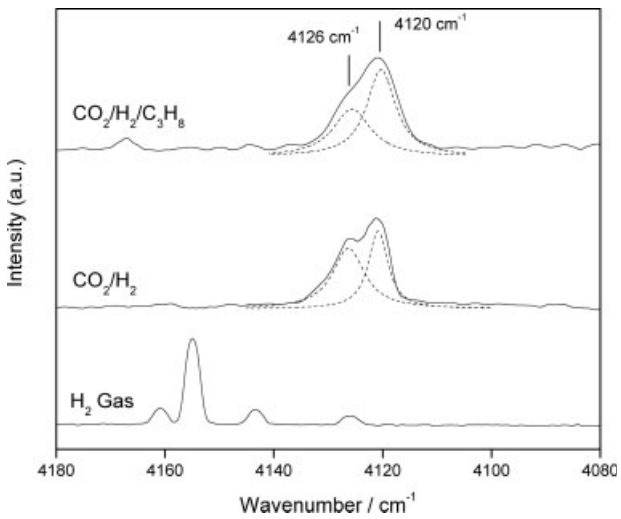

Figure 7. Raman spectra of the vibron region for H_2 gas and H_2 incorporated into hydrates of CO_2/H_2 and $CO_2/H_2/C_3H_8$.

The spectrum of H_2 gas was recorded at room temperature, whereas that of H_2 in the hydrate phase was recorded at liquid nitrogen temperature. It is noted that CO_2/H_2 mixture forms structure I hydrate where as $CO_2/H_2/C_3H_8$ mixture forms structure II hydrate.

Even though Raman spectroscopy shows the presence of different gases in hydrate cages it fails to 1) provide the ratio of CO_2 in large and small cages, and (2) determine whether H_2 is present as a single molecule in the small cages of structure I and structure II or as a cluster of two H_2 molecules. In this study, infrared spectroscopy was used to identify CO_2 in large and small cages in the hydrate structure and NMR spectroscopy was used to determine the hydrogen occupancy in the hydrate cages. Generally, it is agreed that for pure CO_2 hydrate, CO_2 molecules occupy essentially all of the large cages in structure I as well as a fraction (60–80%) of the small cages.[37] However, unlike methane hydrate where the peaks of methane in the small and large cages are separated by almost ten wave numbers,[39] Raman spectroscopy does not show a split peak for CO_2 in large and small cages. On the other hand, FTIR work by Fleyfel and Devlin[38] conducted at lower-temperature indicated two separate peaks of CO_2 in large and small cages in sI and sII hydrates of CO_2.

Pure CO_2 hydrate was synthesized for this study to find the frequencies for CO_2 in the small and large cages. Infrared active asymmetric stretching of CO_2 molecules for pure CO_2 hydrate in the smaller 5^{12} cages and the larger $5^{12}6^2$ cages appears at, 2,347 cm^{-1} and 2,337 cm^{-1}, respectively at $-50°C$. These two modes compare well with the earlier results.[38] A gas mixture of 20% C_3H_8 and the remainder CO_2 was used to form hydrate such that all the large $5^{12}6^4$ cages were occupied by C_3H_8 molecules (see Figure 8), and the smaller 5^{12} cages of the resultant structure II hydrate by CO_2. As seen in Figure 8, the peak position of CO_2 in the smaller cages of structure II appears at, 2,346 cm^{-1}, which suggests an infrared peak position for CO_2 occupying the small cages of structure I, and structure II appears at about 2,346 cm^{-1} at $-50°C$. The recorded spectra for binary CO_2/H_2 hydrate in the 2,250–2,400 cm^{-1} region is shown in Figure 8a. The peak with a shoulder shows the presence of CO_2 in the hydrate cages (asymmetric stretching of CO_2 molecule). The spectral traces are deconvolved, which results in two peaks, one larger peak at 2,337 cm^{-1} indicating the presence of CO_2 in the large cages and a relatively smaller peak at 2,346 cm^{-1} showing the presence of CO_2 in the small cages. Looking at the integrated area under each peak, it is clear that most of the CO_2 in the hydrate phase is present in the larger $5^{12}6^2$ cages (peak at 2,337 cm^{-1}), and a very small amount of CO_2 is present in the small cages of the resultant structure I hydrate (peak at 2,346 cm^{-1}). Based on previous observations on CO_2 hydrate and the results obtained by infrared spectroscopy it can be said that almost 100% of the large cages are occupied by CO_2, and the small cages are mainly occupied by H_2. Figure 8b shows the asymmetric stretching of CO_2 in the ternary mixture of CO_2/H_2/C_3H_8 hydrate. Again the spectral traces are deconvolved into two peaks, one larger peak at 2,337 cm^{-1} showing the presence of CO_2 in the large $5^{12}6^4$ cages and a smaller but significant peak at 2,346 cm^{-1}, a signature of CO_2 in the small 5^{12} cages. Looking at the integrated peak intensities for CO_2 from both systems (binary and ternary hydrates, Figure 8a and b, respectively) it can be said that in the ternary hydrate CO_2 occupies a higher percentage of small cages as compared to the binary hydrate. With just 2.6% C_3H_8 in the CO_2/H_2/C_3H_8 gas mixture the large cages in the resulting structure II hydrate are shared by C_3H_8 and CO_2, and a significant amount of CO_2 occupies the smaller 5^{12} cages, along with H_2. In the binary hydrate CO_2 occupies all of the large cages, and a very small amount of CO_2 actually goes into the small cages, leaving a large number of small cages for H_2.

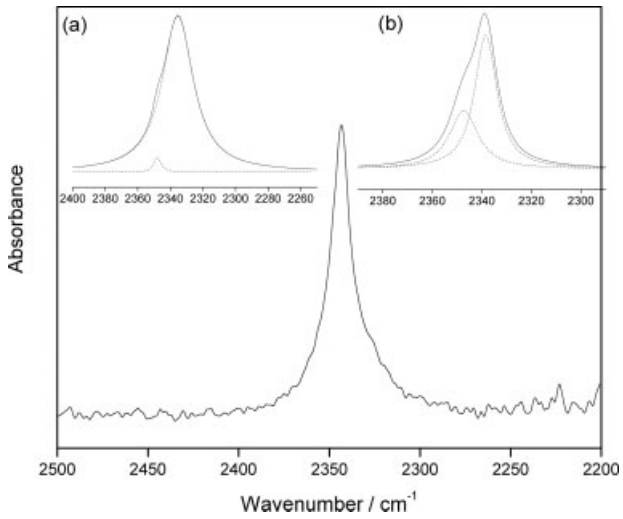

Figure 8. FTIR spectrum of CO_2 (peak at 2346 cm^{-1}) in the small cages of CO_2/C_3H_8 hydrate (large cages are fully occupied by propane) insets (a) the CO_2 peak in small and large cages of CO_2/H_2 hydrate (large cages fully occupied by CO_2), and (b) CO_2 peak in small and large cages of CO_2/H_2/C_3H_8 hydrate (CO_2 shares large cages with C_3H_8 and small cages with H_2).

^{13}C MAS NMR confirmed that the hydrate prepared from the CO_2/H_2 mixture is structure I as was found by PXRD. Only one signal (isotropic shift 124.95 ppm) can be resolved in the ^{13}C MAS spectrum for CO_2/H_2 hydrate. The observed spectral pattern is characteristic of chemical shift anisotropy (CSA), as one may expect for pure CO_2 hydrate in sI,[40] where the spectrum reflects partial averaging of the CSA tensor for CO_2 in the anisotropic environment of the sI large cage at low-temperature.[37,40,41] In this study for the CO_2/H_2 hydrate sample, ^{13}C MAS spectra show that the total integrated intensity of the CO_2 signal corresponds to $2.74 \pm 0.35 \times 10^{21}$ CO_2 molecules per gram of hydrate, which is very close to complete occupancy of the large cages. This leaves a large number of small cages that can be filled with hydrogen in agreement with results obtained by infrared spectroscopic data for CO_2/H_2 hydrate.

In the case of hydrate prepared from the CO_2/H_2/C_3H_8 mixture at 3.8 MPa, a structure II hydrate is formed which is reflected in its ^{13}C spectrum (Figure 9). The two closely spaced and most intense signals at 17.25 and 16.8 ppm are from the methyl (CH_3) and methylene carbon (CH_2) groups of propane in the large cages, respectively. The intensity of the signals corresponds to 6.92×10^{20} C_3H_8 molecules per gram of hydrate, which is less than the number required for full occupancy of the large cages. The remaining large cages have to be occupied by CO_2 in order to form a stable hydrate, considering that complete filling of the large cages

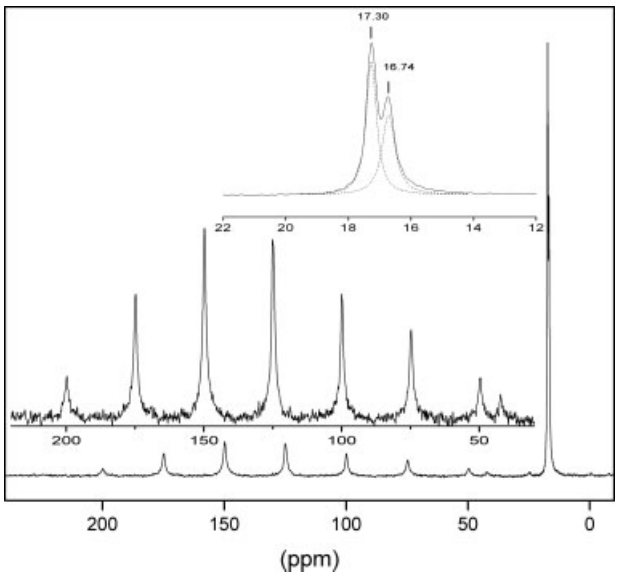

Figure 9. ^{13}C CP MAS NMR spectra for $CO_2/H_2/C_3H_8$.

Upper inset shows the expanded signal of C_3H_8 in large cages of resultant SII hydrate. T = 173K, spinning speed of 2,500 Hz.

in sII is a criterion for stability. The signal of CO_2 appears as a center band and a set of spinning sidebands (similar to CO_2/H_2 hydrate) with an isotropic shift of 125.06 ppm. The spectral pattern is once more indicative of the partially averaged CSA tensor for CO_2 in the small cages plus a contribution from the isotropic resonance for CO_2 in the large cage.[40] The intensity of the CO_2 signal in this hydrate corresponds to 1.7×10^{21} CO_2 molecules per gram of hydrate, which is lower than the total amount of CO_2 present in the hydrate cages of CO_2/H_2 hydrate.

Figure 10 shows a ^1H MAS spectrum of CO_2/H_2 hydrate in D_2O recorded as a spinner-synchronized spin-echo. Three signals can be seen in the spectrum. The broader line at 6.59 ppm, based on its position and its presence in the spectrum of pure CO_2/D_2O hydrate, can be assigned to the residual protons in the D_2O that was used in the hydrate preparation to reduce the intensity of the water proton signal. A prominent signal at 4.26, and a shoulder at 4.09 ppm are from H_2 molecules trapped in the hydrate cages. The assignment is based on the chemical shift of the signals, which is close to the shift of molecular hydrogen. This is also supported by the slow decrease of the signal intensity with the time.[42] The latter likely is due to decomposition of hydrate at 173 K. In the course of three hours, the combined intensity of the two signals was reduced by about 30%. Integration of the spectrum gives the relative intensities of the H_2 signals as 3:1.[42] As mentioned previously, at ambient conditions hydrogen molecules exist in the form of two-spin isomers ortho- and para- hydrogen, with only the ortho-isomer being observable by proton NMR. There have been very few studies regarding ortho- and para- hydrogen in hydrates[28,43] and quantitative studies have not been carried out on spin conversion between ortho- and para- states. Since only the ortho-isomers are being observable by proton NMR, it is possible that the signals at 4.09 and 4.26 ppm in Figure 10 originate from H_2 molecules in singly and doubly occupied small cages as all the large cages are filled by CO_2. It is not surprising that ^1H MAS spectra shows evidence of doubly occupied (two H_2 molecules) small cages. Based on ^1H MAS NMR spectra Kim and Lee[12] have also reported double occupancy of H_2 in the small cages of CO_2/H_2 hydrate. However, they observed a single resonance at 4.2 ppm. In our work, two peaks differing by 0.16 ppm were seen and this is in close agreement with the calculations of Alavi et al.[45] who reported a difference of 0.1 ppm in the peak position of doubly occupied H_2 to that of singly occupied H_2 in the small cages. Considering that the small cage in structure I hydrate have a slightly different shape than those in structure II hydrate, there are possibilities that in CO_2/H_2 hydrate a number of small cages are occupied by two H_2 molecules. So far, there is no convincing evidence of doubly occupied small cages except that from the NMR assignments.

Figure 11 shows a ^1H MAS spectrum of hydrate prepared from $CO_2/H_2/C_3H_8$ mixture at 3.8 MPa. The two most intense signals at 0.64 and 1.07 ppm with relative intensity ratio 3:1 are from CH_3 and CH_2 groups of propane occupying the large cage. No signal from residual protons in D_2O was observed in this sample. The difference likely can be attributed to a difference in dynamic states of the water molecules in the hydrates with the water in the CO_2 hydrate being more mobile and hence giving greater averaging of dipolar couplings and a sharper ^1H resonance. The third signal in the spectrum at 3.93 ppm can be assigned to molecular hydrogen in the hydrate cage. Small cages are the most likely location for this hydrogen since the large cages in this hydrate are well occupied by C_3H_8 and CO_2 (see ^{13}C data). Based on the peak position at 3.93 ppm and the broad nature of the peak we cannot comment on the presence of doubly occupied small cages in this structure II hydrate. Moreover, comparing the absolute intensity of the H_2 peak at 3.93 ppm with that of the C_3H_8 peak in the same hydrate, the

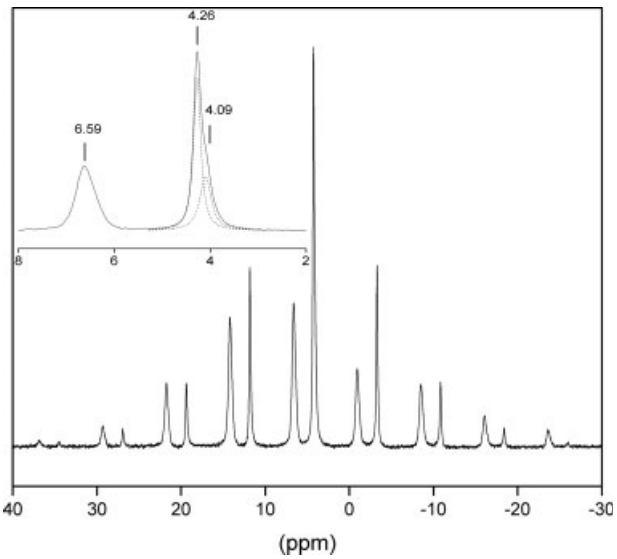

Figure 10. ^1H MAS (T = 173 K, 3,000 Hz) of CO_2/H_2 hydrate prepared in D_2O.

The inset shows the expanded central region of the spectrum without spinning sidebands. The peak at 6.59 ppm is due to the proton impurity in D_2O.

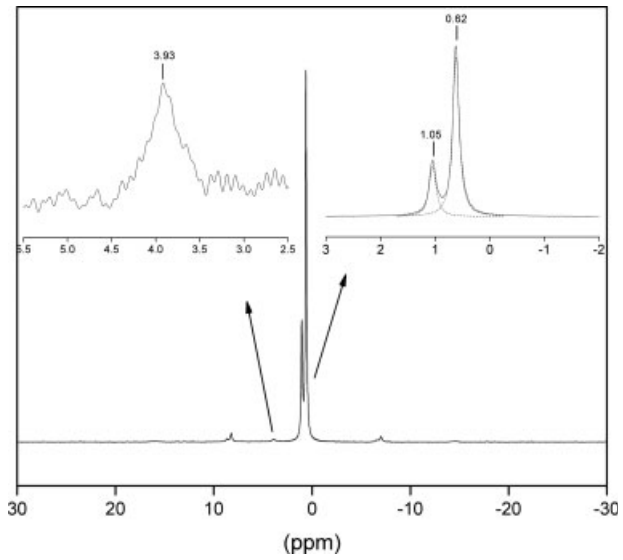

Figure 11. ^{1}H MAS (T = 173 K, 3,000 Hz) of $CO_2/H_2/C_3H_8$ hydrate in D_2O.

Expanded signals for propane are shown on the right inset along with a weak signal from H_2 on the left inset.

hydrogen is present at about 11-12 mol % of the enclathrated propane. This is significantly less than what is found from gas hydrate decomposition just after hydrate synthesis. This difference likely is due to H_2 leaking from the hydrate cages over a period of time on storage and during the NMR analysis at 173 K.[29,44]

Determination of cage occupancy

In most cases NMR can provide accurate quantitative data on cage occupancies. For example, ^{13}C NMR spectra of methane hydrate consist of two well-separated signals at −8.2 ppm (large cage), and −4.3 ppm (small cage), which can be accurately integrated.[39] Previously it was found that the difference in the isotropic chemical shifts of CO_2 in large and small cage of CO_2 hydrate is very small and ^{13}C MAS NMR[37,40,41] cannot separate the signals. We attempted to obtain the relative occupancies by acquiring static powder patterns on a sample of hydrate synthesized with ^{13}C-enriched $CO_2/H_2/D_2O$. However, due to the broadness of the ^{13}C HPDEC (high-power proton decoupling) pattern at −100°C, the CO_2 lines in the large and small cages could not be separated. The static pattern at −40°C was resolved better, but as mentioned earlier CO_2/H_2 hydrate is not stable at that temperature, and, hence, the result was discarded. In the case studied for both binary and ternary hydrate, ^{13}C MAS spectra do not show peak separation sufficient for distinguishing CO_2 in small and large cages of the hydrate. In the absence of distinct signals for CO_2 in small and large cages the use of the statistical thermodynamics[39] approach for absolute occupancy of CO_2 in small and large cavities could not be used. Nevertheless, with the help of known hydrate phase composition from gas chromatography and the information obtained by NMR; an estimate can be made about cage occupancy values for each gas in the hydrate cage. For CO_2/H_2 hydrate which forms structure I, NMR results suggest that $2.74 \pm 0.35 \times 10^{21}$ CO_2 molecules are present in every gram of hydrate (~0.21 gram of CO_2 per gram of hydrate). Assuming that all of the large cages of hydrate have to be filled for a stable CO_2/H_2 hydrate it can be said that in binary CO_2/H_2 hydrate 100% of the large cages (within experimental error) are occupied by CO_2. This result is somewhat similar to the result we obtain by infrared spectroscopy (Figure 8a) where we see most of the CO_2 is present in the large cages. However, Figure 8a also shows a small peak (at 2,346 cm^{-1}) for CO_2 in the small cages. Given the error of $\pm$ 0.35 $\times$ 10^{21} CO_2 molecules in our NMR results it is possible that some of the small cages of CO_2/H_2 hydrate are actually occupied by CO_2. In order to see the cage distribution of H_2 we need to look at the ^{1}H MAS spectra of CO_2/H_2 hydrate in D_2O. As discussed earlier (Figure 10), H_2 molecules occupy only the small cages, both with single and double occupancies. We assign the signal at 4.09 ppm to single and 4.26 ppm to doubly occupied cages.[45] The ratio of hydrogen present in a doubly occupied cavity shows a peak three times stronger than the peak from single hydrogen molecule in the hydrate structure. In addition to the NMR results, we know that hydrate phase composition from gas chromatography suggests that the binary hydrate consists of 92 mol% CO_2 and 8 mol% H_2 (Table 1). Using the information from gas chromatography, as well as from NMR spectra for the cage occupancy calculation, CO_2 occupies 100% of the large cages, whereas 9.3% of the small cages are occupied by bimolecular H_2 and 6.2% by single H_2 molecules (see supplementary section for details of calculation).

The hydrate from the $CO_2/H_2/C_3H_8$ mixture at 3.8 MPa is structure II. Figure 9 shows the ^{13}C spectrum of the $CO_2/H_2/C_3H_8$ hydrate. Two closely spaced signals at 17.25 and 16.8 ppm with the intensity ratio of 2:1 are from CH_3 and CH_2 groups of propane in the large cages. The integral intensity of the signals corresponds to 6.92 x 10^{20} C_3H_8/g (0.05 gram C_3H_8 per gram of hydrate), which is about 43% of the large cages filled for this hydrate. The CO_2 molecules occupy the remaining 57% of the large cages. For the same hydrate, the total intensity of the CO_2 signal corresponds to 1.7×10^{21} CO_2/g (0.124 gram of CO_2 per gram of hydrate). Since close to 0.068 grams of CO_2 is present in the large cages the rest (0.056 gram of CO_2) occupies the small cages,

Table 2. Estimate of Cage Occupancy Values Obtained by Combination of Results from Infrared spectroscopy, Gas Chromatography and NMR. θ'_S Represents Doubly Occupied Cages

		H_2		CO_2		C_3H_8	Hydration number
Description	Hydrate structure	θ_S	θ'_S	θ_S	θ_L	θ_L	n
CO_2/H_2	sI	0.062	0.093	0.000	1.000	0.000	7.09
$CO_2/H_2/C_3H_8$	sII	0.006	0.000	0.340	0.570	0.430	10.05

which is equivalent to 34.0 % of the small cage occupancy (Details of the calculation are given in the supplementary information). Therefore, the NMR results suggest that the large cages are occupied with CO_2 and C_3H_8 and CO_2 also occupies 34% of the small cages. Qualitative information from Infrared spectroscopy also shows that CO_2 occupies a significant number of small cages in the ternary hydrate (Figure 8b). For the H_2 distribution over the hydrate cages, as mentioned earlier, the amount of H_2 in the hydrate is $\sim$12 mol % ($\sim$0.0003 g) of the total amount of propane (Figure 11) which is equivalent to 0.3% of the small cage occupancy. This does not match with the hydrate phase composition obtained by gas chromatography as shown in Table 1. It has been reported previously that H_2 can leak through the hydrate cages on storage.[29,44] Also, NMR only detects ortho-hydrogen in the hydrate cages which can result in an up to two-fold underestimation of the actual amount of H_2 in the hydrate cages.[27,43] Therefore, the cage occupancy of H_2 in the small cages is greater than 0.6%. The cage occupancy values are reported in Table 2 for CO_2/H_2 and $CO_2/H_2/C_3H_8$ hydrate along with the hydration number. The equation used to calculate the hydration number is given elsewhere.[39]

Conclusions

In this work, structural and compositional characterization was carried out on hydrate samples formed from CO_2/H_2 and $CO_2/H_2/C_3H_8$ gas mixtures using PXRD, ^{1}H MAS NMR (with rotor synchronized spin echoes), ^{13}C MAS NMR, mass spectrometry, FTIR (with attenuated total reflection) and Raman spectroscopy. The information obtained enabled the determination of hydrate composition and cage occupancy. Gas hydrates made from (40/60 mol %) CO_2/H_2 mixtures form structure I hydrate at 8.0 MPa. It was found that the large cages are almost fully occupied by carbon dioxide and the small cages were mainly occupied by hydrogen. Furthermore, NMR results suggest that 9.3% of the small cages are occupied by bimolecular H_2 and 6.2% by single H_2 molecules. It was observed that CO_2/H_2 hydrate shows self-preservation on hydrate decomposition. In a CO_2/H_2 separation process via gas hydrate formation an additive like propane reduces the hydrate formation pressure without compromising the CO_2 recovery. It was found that by introducing 2.6% C_3H_8 in CO_2/H_2 gas mixtures the ternary mixture forms pure structure II hydrate at 3.8 MPa. In the resultant hydrate CO_2 (57 %) and C_3H_8 (43 %) share the large cages and a significant portion of small cages is occupied by CO_2 (34 %). Based on the results obtained from this work it can be said that hydrogen occupies the small cages of structure I, as well as structure II hydrate. FTIR was found to be a very important tool to suggest the occupancy ratio of CO_2 in the small and large cages, which otherwise is a very difficult to obtain parameter by Raman/NMR spectroscopy

Acknowledgements

The financial support from the Natural Sciences and Engineering Research Council of Canada (NSERC) and Natural Resources Canada is greatly appreciated. We also thank Dr. Sergey Mitlin for his kind help with mass spectrometer analysis.

Literature Cited

1. Davidson DW. *Gas Hydrates. In Water: A Comprehensive Treatise*. Frank F, ed. New York: Plenum Press; 1973;2:115.
2. Mao WL, Mao H-K, Goncharov AF, Struzhkin VV, Guo Q, Hu J, Shu J, Hemley RJ, Somayazulu M, Zhao Y. Hydrogen clusters in clathrate hydrate. *Science*. 2002;297:2247–2249.
3. Mao WL, Mao H. Hydrogen storage in molecular compounds. *Proc Nat Acad Sci USA*. 2004;101:708–710.
4. Klara SM, Srivastava, RD. US DOE integrated collaborative technology development program for CO_2 separation and capture. *Environ Prog*. 2002;21:247–253.
5. Joshi MM, Lee SG. Integrated gasification combined cycle - A review of IGCC technology. *Energy Sources.* 1996;18:537–568.
6. Linga P, Kumar R, Englezos P. Capture of Carbon dioxide from conventional power plants or from integrated gasification plants through gas hydrate formation/dissociation. *J Energy Climate Change*. 2006;1:75–82.
7. Linga P, Kumar R, Englezos P. The clathrate hydrate process for post and pre-combustion capture of carbon dioxide. *J Hazard Mater*. 2007;149:625–629.
8. Linga P, Adeyemo A, Englezos P. Medium-pressure clathrate hydrate/membrane hybrid process for postcombustion capture of carbon dioxide. *Environ Sci Technol*. 2007;42:315–320.
9. Kumar R, Linga P, Ripmeester JA, Englezos, P. A two-stage clathrate hydrate membrane process for pre-combustion capture of carbon dioxide and hydrogen. *J Environ Eng*. accepted September 14, 2008. In press (doi:10.1061/(ASCE)EE. 1943-7870.0000002).
10. Kumar R, Wu HJ, Englezos P. Incipient hydrate phase equilibrium for gas mixtures containing hydrogen, carbon dioxide and propane. *Fluid Phase Equilibria*. 2006;244:167–171.
11. Linga P, Kumar R, Englezos P. Gas hydrate formation from hydrogen/carbon dioxide and nitrogen/carbon dioxide gas mixtures. *Chem Eng Sci*. 2007;62:4268–4276.
12. Kim D-Y, Lee H. Spectroscopic identification of the mixed hydrogen and carbon dioxide clathrate hydrate *J Am Chem Soc*. 2005;127: 9996–9997.
13. Sugahara T, Murayama S, Hashimoto S, Ohgaki K. Phase equilibria for $H_2 + CO_2 + H_2O$ system containing gas hydrates. *Fluid Phase Equilibria*. 2005;233:190–193.
14. Sugahara T, Mori H, Sakamoto J, Hashimoto S, Ogata K, Ohgaki K. Cage occupancy of hydrogen in carbon dioxide, ethane, cyclopropane, and propane hydrates. *Open Thermodynamics J*. 2008;2:1–6.
15. Florusse LJ, Peters CJ, Schoonman J, Hester KC, Koh CA, Dec SF, Marsh KN, Sloan ED. Stable low-pressure hydrogen clusters stored in a binary clathrate hydrate. *Science*. 2004;306:469–471.
16. Lee H, Lee J-W, Kim DY, Park J, Seo Y-T, Zeng H, Moudrakovski IL, Ratcliffe CI, Ripmeester JA. Tuning clathrate hydrates for hydrogen storage. *Nature*. 2005;434:743–746.
17. Hashimoto S, Murayama S, Sugahara T, Ohgaki K. Phase equilibria for $h_2 + co_2$ + tetrahydrofuran + water mixtures containing gas hydrates. *J Chem Eng Data,* 2006;51:1884–1886.
18. Struzhkin VV, Militzer B, Mao WL, Mao H-K, Hemley RJ. Hydrogen storage in molecular clathrates. *Chem Rev*. 2007;107:4133–4151.
19. Lokshin KA, Zhao Y, He D, Mao WL, Mao H, Hemley RJ, Lobanov MV, Greenblatt M. Structure and dynamics of hydrogen molecules in the novel clathrate hydrate by high pressure neutron diffraction. *Phys Rev Lett*. 2004;93:125503–1.
20. Strobel TA, Taylor CJ, Hester KC, Dec SF, Koh, CA, Miller KT, Sloan ED. Molecular hydrogen storage in binary thf−h2 clathrate hydrates. *J Phys Chem B*. 2006;110:17121–17125.
21. Hester KC, Strobel TA, Sloan ED, Koh CA, Huq A, Schultz AJ. Molecular hydrogen occupancy in binary THF−H_2 clathrate hydrates by high resolution neutron diffraction. *J Phys Chem B*. 2006;110:14024–14027.
22. Anderson R, Chapoy A, Tohidi B. Phase relations and binary clathrate hydrate formation in the system H_2−THF−H_2O. *Langmuir*. 2007;23:3440–3444.
23. Strobel TA. On some clathrates of hydrogen. PhD Thesis. Colorado School of Mines, Golden, CO; 2008.
24. Patchkovskii S, Tse JS. Thermodynamic stability of hydrogen clathrates. *Proc Nat Acad Sci USA*. 2003;100:14645–14650.
25. Sluiter MHF, Adachi H, Belosludov RV, Belosludov VR, Kawazoe Y. Ab initio study of hydrogen storage in hydrogen hydrate clathrates. *Mater Trans*. 2004;45:1452–1454.

26. Alavi S, Ripmeester JA, Klug, DD. Molecular dyanmics study of structure II hydrogen clathrates. *J Chem Phys*. 2005;123:024507.
27. Kumar R, Lang S, Moudrakovski IL, Englezos P, Ripmeester JA. Spectroscopic measurement on clathrate hydrates formed by H_2/THF mixtures. In preparation.
28. Senadheera L, Conradi, MS. Rotation and diffusion of H_2 in hydrogen-ice Clathrate by ^{1}H NMR. *J Phys Chem B*. 2007;111:12097–12102.
29. Alavi S, Ripmeester JA. Hydrogen-gas migration through clathrate hydrate cages. *Angew Chem Int Ed*. 2007;46:6102–6105.
30. Murphy PJ, Roberts S. Laser Raman spectroscopy of differential partitioning in mixed-gas clathrates in H_20-CO_2-N_2-CH_4 fluid inclusions: Implications for microthermometry Geochim. *Cosmochim. Acta*. 1995;59:4809–4824.
31. Wang X, Schultz AJ, Halpern Y. Kinetics of methane hydrate formation from polycrystalline deuterated ice. *J Phys Chem A*. 2002; 106:7304–7309.
32. Susilo R, Moudrakovski IL, Ripmeester JA, Englezos P. Hydrate kinetics study in the presence of nonaqueous liquid by nuclear magnetic resonance spectroscopy and imaging. *J Phys Chem B*. 2006; 110:25803–25809.
33. Moudrakovski IL, Ratcliffe CI, McLaurin GE, Simard B, Ripmeester JA. Hydrate Layers on Ice Particles and Superheated Ice: a ^{1}H NMR microimaging study. *J Phys Chem A*. 1999;103:4969–4972.
34. Susilo R, Ripmeester JA, Englezos P. Methane conversion rate into structure H hydrate crystals from ice. *AIChE J*. 2007;53:2451–2460.
35. Henning RW, Schultz AJ, Thieu V, Halpern Y. Neutron diffraction studies of co_2 clathrate hydrate: formation from deuterated ice *J Phys Chem A*. 2000;104:5066–5071.
36. Takeya S, Ripmeester JA. Dissociation behavior of clathrate hydrates to ice and dependence on guest molecules. *Angew Chem*. 2008;120:1296–1299.
37. Udachin KA, Ratcliffe CI, Ripmeester JA. Structure, composition, and thermal expansion of CO_2 hydrate from single crystal X-ray diffraction measurements. *J Phys Chem B*. 2001;105:4200–4204.
38. Fleyfel F, Devlin JP. Carbon dioxide clathrate hydrate epitaxial growth: Spectroscopic evidence for formation of the simple Type-II CO_2 hydrate. *J Phys Chem*. 1991;95:3811–3815.
39. Kumar R, Linga P, Moudrakovski IL, Ripmeester JA, Englezos, P. Structure and kinetics of gas hydrates from methane/ethane/propane mixtures relevant to the design of natural gas hydrate storage and transport facilities. *AIChE J*. 2008;54:2132–2144.
40. Ratcliffe CI, Ripmeester JA. ^{1}H and ^{13}C NMR studies on carbon dioxide hydrate. *J Phys Chem*. 1986;90:1259–1263.
41. Ripmeester JA, Ratcliffe CI. The diverse nature of dodecahedral cages in clathrate hydrates as revealed by ^{129}Xe and ^{13}C NMR spectroscopy: CO_2 as a small-cage guest. *Energy Fuels*. 1998;12:197–200.
42. Moudrakovski I, Luzi M, Kumar R, Lu H, Ripmeester J. Experimental solid state nmr of gas hydrates: problems and solutions. 6th International Conference on Gas Hydrate; 6–10 July 2008; Vancouver, BC, Canada.
43. Ulivi L, Celli M, Giannasi A, Ramirez-Cuesta AJ, Bull DJ, Zoppi M. Quantum rattling of molecular hydrogen in clathrate hydrate nanocavities. *Phys Rev B*. 2007;76:161401(1)–161401(4).
44. Okuchi T, Moudrakovski IL, Ripmeester JA. Efficient storage of hydrogen fuel into leaky cages of clathrate hydrate. *Appl Phys Lett*. 2007;91:171903(1)–171903(3).
45. Alavi S, Ripmeester JA, Klug, DD. NMR shielding constant for hydrogen guest molecules in structure II clathrates. *J Chem Phys*. 2005;123:051107.
46. Ohno H, Hondoh T. Micro-Raman Study of Air Clathrate Hydrates in Polar Ice from Dome Fuji, Antarctica. Physics and Chemistry of ice. Proceedings of the 11th International Conference on the Physics and Chemistry of Ice; 23–28 July, 2006; Bremerhaven, Germany. Werner F. Kuhs, ed. The Royal Society of Chemistry, Cambridge, U.K; 2007:459.

Manuscript received Oct. 1, 2008, and revision received Jan. 12, 2009.